Plasmonic properties of gold nanoparticle clusters formed via applying AC electric field

doi: 10.1039/C8SM00097B

Soft Matter, Vol.14 (25 March 2018)
[DOI: 10.1039/c8sm00097b]

The plasmonic properties of gold nanoparticle clusters formed Via applying an AC electric field

Kanako WATANABE, Eri TANAKA, Haruyuki ISHII and Daisuke NAGAO

Department of Chemical Engineering, Tohoku University

Abstract

An external electric AC field with a field strength ranging from 10 V mm^{-1} to 30 V mm^{-1} and a frequency ranging from 0.1 kHz to 1 MHz was applied to suspensions of gold nanoparticles (Au NPs) to control their plasmonic properties. Apparent differences in the UV-vis spectra of the Au NPs were observed between the spectra with and without the field application. The characteristic red color of the Au NP suspension darkened; this suggested that the application of the AC field caused the aggregation of the Au NPs. In addition, the sizes of the Au NP clusters in suspension formed by the AC field application depended on the frequency of the applied field. The surface-enhanced Raman scattering (SERS) effects of Au NP clusters were examined by comparing the difference in Raman intensities obtained at 30 V mm^{-1} and in a frequency range of 0.1 kHz to 1 MHz. The application of a lowfrequency field at 0.1 kHz caused a rapid aggregation of the Au NPs, resulting in low Raman intensities of the probe molecules. Conversely, high-frequency applications between 1 kHz and 1 MHz successfully enhanced the Raman intensities of the molecules in suspension. The strong correlation of the optical/sensing properties with the Au NP clustering states reveals that the application of an AC electric field is a powerful tool for control over the plasmonic properties.

Electronic supplementary information (ESI) available :

Size distributions and UV-vis spectra of Au NPs before and after the incubation of PMBA, size distributions of the Au NPs in suspensions measured by the field application of 1 MHz in field strengths from 0 V mm^{-1} to 50 V mm^{-1}, size distributions of the Au NPs in suspensions measured by the field application in field strengths from 10 V mm^{-1} to 50 V mm^{-1} in the frequency range from 0.1 kHz to 1 MHz, SEM images of Au NPs on a glass substrate observed by the field application, summary of the relationship between clustering states and the plasmonic properties of Au NPs, size distributions of the Au NPs in suspensions measured by the field application of 1 MHz at 30 V mm^{-1} in the application time from 30 s to 180 s, and UV-vis spectra (a) and size distributions (b) of the Au NPs in suspensions measured by the field application at 30 V mm^{-1} in the frequency 10 kHz and 100 kHz. See DOI: 10.1039/c8sm00097b

1. Introduction

Plasmonic nanoparticles such as silver and gold nanoparticles (Au NPs) have attracted enormous interest in various fields,[1,2] especially optics[3,4] and sensors.[5,6] An electric field that is induced by light irradiation to the surface of plasmonic nanoparticles resonates with the light of a specific wavelength, which is called localized surface plasmon resonance (LSPR). Because the light wavelength depends on the size and shape, control over morphology is one of the big challenges for developing optical materials. Spherical Au NPs are well-known to exhibit size-dependent color.[7] Gold nanorods,[8,9] gold nanoplates,[10] and gold nanostars[11] have shape-dependent color.

Not only control over morphology but also assembling plasmonic nanoparticles is a promising approach to control their optical properties.[12,13] The LSPR peaks of nanostructured plasmonic metals can be changed via the formation of “hotspots,” which are interstices between adjacent nanostructured plasmonic metals.[14,15] These hotspots also play an important role in surface-enhanced Raman scattering (SERS). SERS has shown great potential for application in highly sensitive sensors, particularly for biomolecules (for example, DNA and viruses)[16–18] since its discovery in the 1970s.[19,20] Previous reports have demonstrated the Raman signal intensity of specific molecules on the surface of nanostructured plasmonic nanoparticles. Lithography has been commonly employed as a down-sizing method to create nanostructured patterns of plasmonic metals on a substrate.[21] The formation of chemical bonds between clustered plasmonic nanoparticles is a bottom-up approach[22–24] for improving the detection sensitivities of molecules.[25,26]

External stimuli such as temperature, pH, and light have recently been employed to provide plasmonic nanoparticles with switchable properties for controlling the assembly states of the nanoparticles.[27] Heating or cooling is a feasible stimulus suitable for controlling the distance between nanoparticles incorporated into thermosensitive polymers.[28,29] Lightinduced clustering of Au NPs has been reported by several groups.[30,31] The application of a magnetic field is another approach to change the distance between gold nanoparticles deposited onto magnetically responsive particles.[32–34] These reports indicate that the plasmonic properties of metal nanoparticles can be controlled by changing their clustering states.

The application of an external field to disperse particles in suspensions is a useful pathway to control the inner structure of the assemblies. For instance, in our previous reports, an external magnetic field was used to control the clustering states of cores incorporated into the assemblies of yolk/shell particles.[35,36] The assembly state of the magnetically responsive inner cores could be changed by a magnetic field applied to a monolayer of yolk/shell particles. In one of our recent reports, the inner core motions of yolk/shell particles were found to be reversibly switched by the application of an electric AC field.[37]

The application of an electric field is another potential technique for local control over the clustering states of Au NPs because of their high responsivity to an AC electric field compared with other nano-sized particles.[38,39] Furthermore, the application conditions for an AC electric field can be altered by changing the operational factors: field strength, frequency, and application time.

The purpose of the present work is to illustrate the relationship between the clustering states and plasmonic properties of Au NPs in suspension. An AC field strength range of 10 V mm^{-1} to 50 V mm^{-1} and a frequency range of 0.1 kHz to 1 MHz were utilized as operational factors for controlling the clustered states of Au NPs because the responsivity of Au NPs has been reported to strongly depend on the application conditions of an electric field.[40] The correlation between the plasmonic properties and Au NP clustering states was investigated using their optical properties with the assistance of the size distribution of Au NPs measured in suspension. The SERS effect of the Au NP clusters was also examined by comparing the difference in Raman intensity with and without an AC electric field.

2. Experimental

2.1 Materials

Hydrogen tetrachloroaurate(III) tetrahydrate ($HAuCl_4 \cdot 4H_2O$, 99.9%), trisodium citrate dihydrate (Na-cit·$2H_2O$, 99%), 4-mercaptobenzoic acid (PMBA, >95.0%), and ethanol (99.5%) were purchased from Wako Pure Chemical Industries (Osaka, Japan).

2.2 Synthetic procedure for increasing the sizes of Au NPs in a seeded growth experiment

Au NPs employed for SERS measurements were synthesized by a seeded growth method using 15-nm Au NPs as seeds.[41] The Au seeds were prepared using the citric reduction method[42] in which $HAuCl_4$ is added to an aqueous solution of Na-cit at 80°C under stirring. The initial concentrations of Na-cit and $HAuCl_4$ were 1.68 mM and 0.24 mM, respectively. The volume of the reaction mixture was 300 mL. Four hours after initiation of the reaction, 270.4 mL of the reactant solution was removed to adjust the number of seeds. To the rest of the reactant solution, 0.2 mL of $HAuCl_4$ solution (25 mM) and 0.2 mL of Na-cit (60 mM) were sequentially injected under stirring at 80°C. Every 30 min, the process of removal and injection was repeated 15 times, resulting in Au NPs with an average size of 38 nm. The concentration of Au in the solution was 1.93 mM.

2.3 Measurements of plasmonic properties after the application of an external AC field

Fig. 1 shows the schematic procedure for obtaining the plasmonic properties of a Au NP suspension to which an external AC field was applied before measurement. The suspension was injected into a channel formed using double-sided tape on a glass substrate. An external AC field was applied to the Au NP suspension using a function generator (GW Instek, SFG-2004) and an amplifier (NF Circuit Design Bloc, HSA4011). The electric field strength (peak to peak) was measured using a digital oscilloscope (GW Instek, GDS-1062A). An AC field strength range of 10 V mm^{-1} to 50 V mm^{-1} and a frequency range of 0.1 kHz to 1 MHz were used for the field application. After the application of the field, UV-vis spectra and dispersion particle sizes of the Au NPs in suspension were measured via a UV-vis spectrometer (Hitachi, U-3900) and a dynamic light scattering (DLS) photometer (Otsuka Electronics Co., ELSZ-2), respectively. To obtain the data of UV-vis and DLS, the Au NPs to which an AC field was applied with the setup shown in Fig. 1 were transferred into cuvettes, used in UV-vis and DLS measurements.

2.4 Raman measurements of PMBA after the application of an external AC field

PMBA in ethanol was mixed into the suspension of Au NPs and incubated for 2 h. The concentration of PMBA was 10^{-6} M. As shown

in Fig. S1 (ESI†), the DLS peaks and UV-vis spectra of the Au NP suspension changed marginally after the addition of PMBA. After the application of an AC field at 30 V mm^{-1} in the frequency range of 0.1 kHz to 1 MHz for 60 s, Raman spectra were recorded using a microscopic laser Raman spectrometer (JASCO, NRS-500). Measurements with a 50 × objective lens were performed using a 785 nm laser with a 10.9 mW incident power and an integration time of 60 s. The Raman measurements above were repeated at least three times.

2.5 Characterization

The Au NPs were observed using FE-TEM (Hitachi, HD-2700). The Au NP assemblies formed by applying an AC field were observed using SEM (Hitachi, TM-1000S).

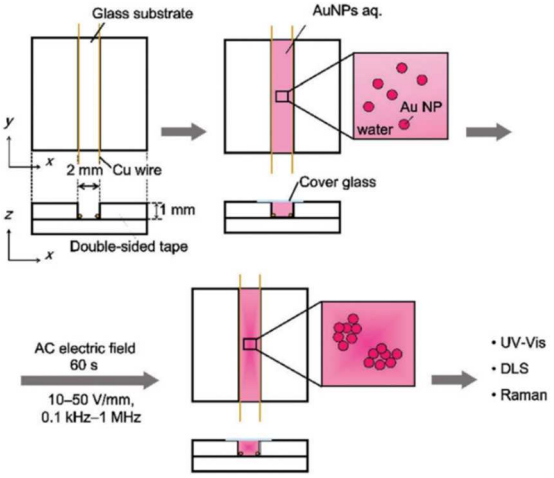

Fig. 1 Schematic procedure for the measurements of the plasmonic properties of Au NPs to which an external AC field was applied before the measurements.

3. Results and discussion

Fig. 2(a) shows a TEM image of the Au NPs obtained from the seeded growth procedure. The coefficient of variation of the Au NPs was 13%. The UV-vis spectrum of the Au NPs in suspension is presented in Fig. 2(b). A single peak, derived from LSPR of the Au NPs, was observed at 530 nm, which is almost identical to the value reported previously.[43]

External AC electric fields in the field strength range of 10 V mm^{-1} to 50 V mm^{-1} were applied to the Au NP suspensions. Fig. 3(a) and (b) show the UV-vis spectra and colors of the Au NPs obtained by field application at 10 V mm^{-1} for 60 s. The spectrum measured without the application of an AC field is also presented. The absence of differences in appearance in Fig. 3(a) and (b) suggests that the dispersion states of the Au NPs were only slightly affected by the field application.

An increase in the electric field strength to 30 V mm^{-1} changed the optical properties of the Au NPs at each frequency. The UV-vis spectra shown in Fig. 3(c) indicated that all of the spectra had an intense peak at approximately 530 nm. The widths of the peaks were broadened by the field application, indicating that the application of the electric fields caused the Au NPs to aggregrate.[44,45] In Fig. 3(d), the characteristic red color was exhibited for suspensions without the application of an AC field. However, the red color observed after the application seemed to be darker than that without the electric field. After the application of a field at 0.1 kHz, the color of the suspension turned black-purple. As shown in Fig. 3(f), more apparent color changes were observed at 50 V mm^{-1} compared with those at other field strengths.

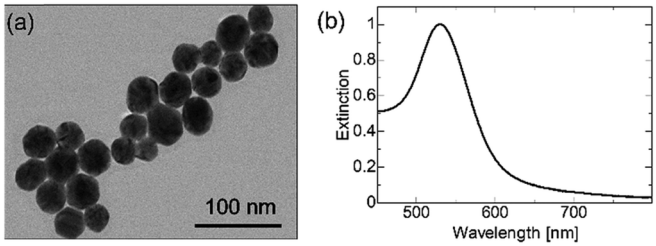

Fig. 2 TEM image of Au NPs (a) and UV-vis spectrum of the Au NPs in suspension (b).

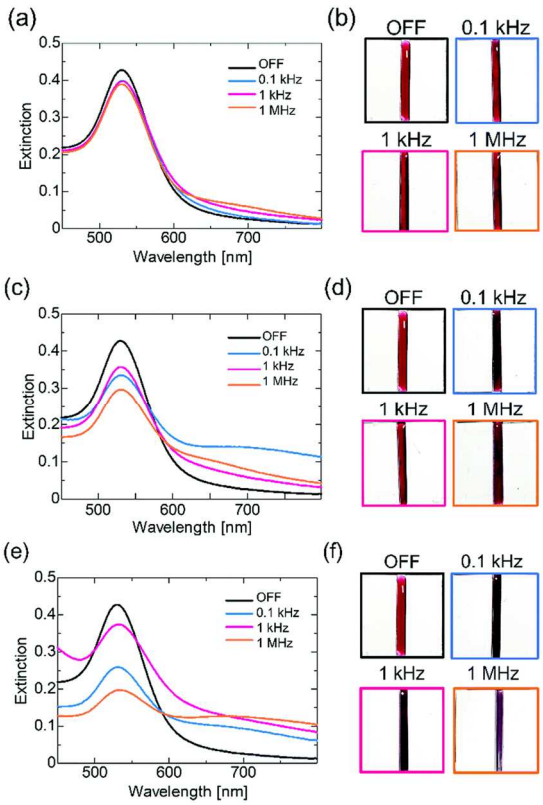

Fig. 3 UV-vis spectra measured in the field frequency range of 0.1 kHz–1 MHz at different strengths of 10 V mm^{-1} (a), 30 V mm^{-1} (c) and 50 V mm^{-1} (e). The spectrum measured without the application of an AC field was also presented in the figures (OFF state). Color of the Au NP suspension observed at 10 V mm^{-1} (b), 30 V mm^{-1} (d) and 50 V mm^{-1} (f) in the same frequency range.

Under the application of an AC field, the dielectric force induces the Au NPs to move in their suspensions. The time average of the dielectric force is given by eqn (1).[40]

$$\langle \vec{F}_{\mathrm{DEP}}(t) \rangle = 2\pi\varepsilon_{\mathrm{m}} a^3 \mathrm{Re}[K(\omega)] \nabla \left| \vec{E}_{\mathrm{rms}} \right|^2 \quad (1)$$

where ε_{m} is the permittivity of the medium, a is the radius of the nanoparticle, and $\vec{E}_{\mathrm{rms}}$ is the rms value of the electric field. $K(\omega)$ in eqn (1) is the Clausius–Mosotti factor given by eqn (2).[40,46]

$$K(\omega) = \frac{\varepsilon_{\mathrm{p}} - \varepsilon_{\mathrm{m}} - \frac{\mathrm{j}}{\omega}(\sigma_{\mathrm{p}} - \sigma_{\mathrm{m}})}{\varepsilon_{\mathrm{p}} - 2\varepsilon_{\mathrm{m}} - \frac{\mathrm{j}}{\omega}(\sigma_{\mathrm{p}} - 2\sigma_{\mathrm{m}})} \quad (2)$$

where ε_{p} is the permittivity of the nanoparticle, $\mathrm{j}^2 \mathrm{is} -1, \omega = 2\pi f$ and f is the frequency. σ_{p} and σ_{m} are the conductivities of the nanoparticles and the medium, respectively. According to eqn (1), the dielectric force is proportional to the field strength squared. As indicated in a previous work,[40] the Clausius–Mosotti factor marginally changes in the frequency range from 0.1 kHz to 1 MHz. As shown in Fig. 3, apparent changes in the optical properties caused by the field application were observed at 30 V mm^{-1} or higher, indicating that the dielectric force could be a factor influencing the assembly of the Au NPs in their suspensions. Fig. S2 (ESI†) shows the size distributions of Au NPs acquired by the application of an electric field with a frequency of 1 MHz and field strengths ranging from 0 V mm^{-1} to 50 V mm^{-1}. The size distributions in Fig. S2 (ESI†) are important data to support the strong correlation between the clustering sizes and the plasmonic properties of the Au NPs in solution. The size of the Au NP clusters increased with the field strength. These results suggest that the field-induced clustering of the Au NPs can be controlled with the field strength as an operational factor.

AC electroosmosis is a force produced by fluid flow along the electrode surface. The fluid velocity near the electrode is given by eqn (3).[47]

$$\langle v \rangle = \frac{1}{8} \frac{\varepsilon V_0^2 \Omega^2}{\eta x (1 + \Omega^2)^2} \quad (3)$$

where V_0 is the potential applied to the electrode, η is the solution viscosity, x is the coordinate axis along the electrode surface with its origin at the center of the electrode gap, and the dimensionless frequency Ω is given by eqn (4).[47]

$$\Omega = \omega x \frac{\varepsilon}{\sigma} \frac{\pi}{2} \kappa \tag{4}$$

where κ is the Debye–Hückel length. Eqn (3) indicates that a strong electroosmotic flow occurred at low frequencies. In addition, surface polarization is dominant at low frequencies because the polarizability of particles depends on the frequency.[48] Surface polarization induced strong interactions between the Au NPs at 0.1 kHz, causing the formation of Au NP clusters.

Fig. S3 to S5 (ESI†) show the size distributions of the Au NPs in suspension, observed after the application of a field for 60 s. Although a single intense peak accompanying a small peak was measured at 10 V mm^{-1} in Fig. S3 (ESI†), bimodal peaks were measured at 30 V mm^{-1} or higher in Fig. S4 and S5 (ESI†). Fig. S6 (ESI†) shows SEM images of Au NPs dried far away from the Cu electrodes on the glass substrate of a Au NP suspension after the application of an electric field of 30 V mm^{-1}. The clustered Au NPs are shown as tiny white dots; higher densities of Au NPs were observed for all of the field applications compared with those without the application, suggesting that the Au NPs formed clusters in their suspensions. Although the cluster formation was affected by capillary forces during the suspension drying process, the excess aggregation of Au NPs was induced by the 0.1 kHz application at 30 V mm^{-1}.

At a high frequency of 1 MHz, the dielectric property of water should be considered.[49,50] The dielectric loss causes the dielectric friction of water, resulting in fluid flow. This flow should lead to Au NP movement, indicating the formation of Au NP clusters. Because the dielectric loss increased with the field strength, rapid aggregation of the Au NPs could have been induced at 50 V mm^{-1} and 1 MHz.

External AC fields at 30 V mm^{-1} in the frequency range of 0.1 kHz to 1 MHz were applied to a PMBA solution in the presence of Au NPs. Fig. 4(a) shows Raman spectra obtained by the field application for 60 s to Au NP suspensions. Almost all of the peaks detected could be attributed to the vibration modes of PMBA.[51,52] None of the peak positions were shifted after the AC field application, regardless of the applied frequency. It should be noted that the intensities of the Raman signals demonstrate frequency dependence. Because the signal intensity of SERS has been reported to be dependent on the Au NP concentration,[53] the Raman spectra of PMBA were measured without an electric field. In the present work, the Raman signal acquired at 0.1 kHz was dramatically decreased compared with that in the OFF state.

Based on the measured Raman intensities, the two intense peaks at 1020 cm^{-1} and 1391 cm^{-1} in the Raman spectra were chosen to compare the SERS enhancements at different AC electric field frequencies. As summarized in Fig. 4(b), the intensities of the two peaks at 0.1 kHz showed the minimum intensities. Conversely, high intensities for the peaks were observed for the field application at 1 kHz or higher. Fig. 4(c) shows the relative intensities of the two peaks to those without AC field application for the suspensions. Although relative intensities in the range of 20% to 50% were obtained at 0.1 kHz, the maximum enhancement in the application at 1 kHz was 150% at 1391 cm^{-1}.

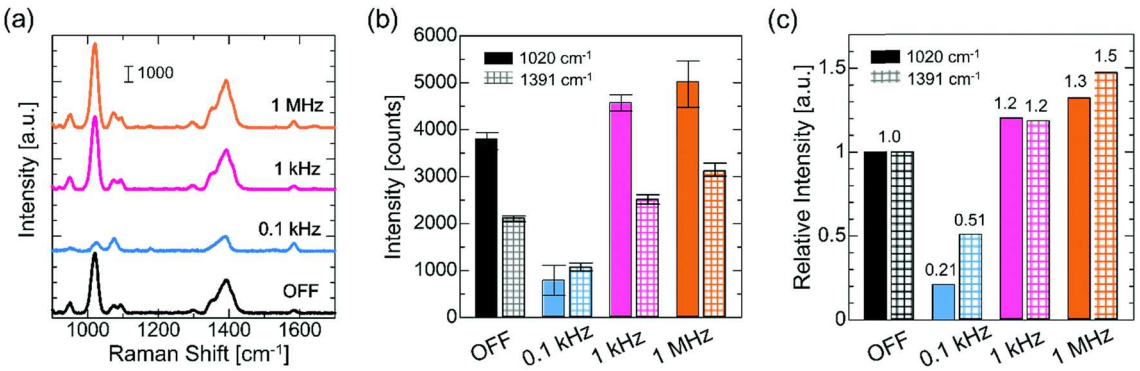

Fig. 4 Raman spectra of PMBA measured by the field application of 30 Vmm^{-1} in the frequency range of 0.1 kHz to 1 MHz (a), their intensities (b) at 1020 cm^{-1} and 1391 cm^{-1} in the Raman spectra and the relative intensities (c) normalized by those obtained at the same wavenumbers without the application of an electric-field (OFF state).

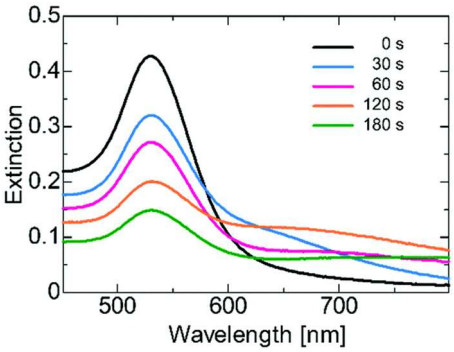

Fig. 5 UV-vis spectra measured by the application of 1 kHz at 30 V mm^{-1} for each application time from 30 s to 180 s.

The SERS enhancements acquired at each frequency can be strongly correlated with the assembly states of the Au NPs in solution. The relationship between the DLS sizes of the Au NPs and the Raman intensities is summarized in Table S1 (ESI†). Due to the fast sedimentation of large Au NP clusters induced by the field application at 0.1 kHz, the concentration of the Au NPs around the center of the Raman measurement cell that the laser focused on could be lower at 0.1 kHz than that without application of the electric field. This is a possible reason why the intensities of PMBA measured under the application at 0.1 kHz were weaker than that without the electric field. On the other hand, the application of 1 kHz or higher caused a moderate clustering of the Au NPs in the suspension, resulting in the formation of hotspots among neighboring Au NPs.

In addition to the field strength and frequency, the application time of an electric field can also be adjusted to change the Au NP cluster sizes in suspension. Fig. 5 shows the UV-vis spectra of the Au NPs observed after field application at 30 V mm^{-1} and 1 MHz for 0 to 180 s. The peaks gradually broadened with application time. The average sizes of the Au NP clusters changed as the time increased as shown in Fig. S7 (ESI†), which shows that the plasmonic properties were controllable by adjusting the application time of the electric field.

To evaluate the reproducibility of the formation of Au NP clusters, we compared the UV-vis spectra of the Au NPs measured after the application of an electric field at 1 MHz at 30 V mm^{-1}. As shown in Fig. 6, the spectra marginally changed in each measurement. The results indicate that accurate control over the clustering states of the Au NPs can be achieved using an external AC electric field. The electric field-induced clustering of Au NPs, however, is irreversible in the present system. We think that coating Au NPs with a thin layer (*e.g.* silica layer) should be effective to overcome the irreversibility and will realize reversible control over the clustering by switching an electric field.

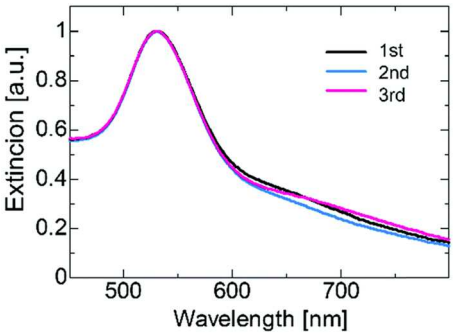

Fig. 6 UV-vis spectra of Au NPs measured by the field application of 1 MHz at 30 V mm^{-1} for 60 s.

4. Conclusion

The plasmonic properties of Au NPs in suspension were compared with and without the application of an external AC field in the field strength range from 10 V mm^{-1} to 50 V mm^{-1} and the frequency range from 0.1 kHz to 1 MHz. The UV-vis spectra broadened with the application of an electric field, suggesting that the Au NPs became clustered. Because the clustering states of the Au NPs depend on the applied field conditions, it was suggested that the clusters were formed by various forces (*e.g.*, dielectrophoresis, AC electroosmosis, particle polarization and the dielectric friction of water). The suspension color and SEM observations of the Au NPs

experimentally supported the frequency-dependent clustering in suspension. No SERS enhancements were observed for the Au NP suspension treated with low-frequency application of an electric field at 0.1 kHz at 30 V mm^{-1}. Conversely, application at high frequencies of 1 kHz or 1 MHz successfully enhanced the Raman intensities by approximately 150%, which was probably due to hotspot formation caused by the clustering of Au NPs. In addition, the clustering states of the Au NPs were controlled by the field application time. The present results show that the application of an external AC electric field may be a promising approach to obtain specific plasmonic properties from metal nanoparticles in suspension. This proposed technique is applicable to developing optical materials and highly sensitive biosensors.

Conflicts of interest

There are no conflicts to declare.

Acknowledgements

The authors thank M. Nemoto for the measurements of Raman spectra, A. Arakawa for the measurements of SEM images and technical support staff in the Department of Engineering, Tohoku University. This research was mainly supported by the Ministry of Education, Culture, Sports, Science and Technology (JSPS KAKENHI Grant numbers 16J03375 and 17H0274440).

Notes and references

[1] V. Amendola, R. Pilot, M. Frasconi, O. M. Maragò and A. M. Iatì, *J. Phys.: Condens. Matter,* 2017, **29**, 203002.

[2] E. Boisselier and D. Astruc, *Chem. Soc. Rev*., 2009, **38,** 1759.

[3] T. Chen and B. M. Reinhard, *Adv. Mater*., 2016, **28**, 3522–3527.

[4] M. B. Cortie and A. M. McDonagh, *Chem. Rev*., 2011, **111**, 3713–3735.

[5] S. Guo and E. Wang, *Nano Today*, 2011, **6**, 240–264.

[6] T. Vo-Dinh, H. N. Wang and J. Scaffidi, *J. Biophotonics*, 2010, **3**, 89–102.

[7] C. J. Orendorff, T. K. Sau and C. J. Murphy, *Small*, 2006, **2**, 636–639.

[8] L. M. Liz-Marza´n, *Nano Today*, 2004, **7**, 26–31.

[9] C. J. Murphy, T. K. Sau, A. M. Gole, C. J. Orendorff, J. Gao, L. Gou, S. E. Hunyadi and T. Li, *J. Phys. Chem. B*, 2005, **109**, 13857–13870.

[10] S. P. Chandran, M. Chaudhary, R. Pasricha, A. Ahmad and M. Sastry, *Biotechnol. Prog*., 2006, **22**, 577–583.

[11] C. G. Khoury and T. Vo-Dinh, *J. Phys. Chem. C*, 2008, **112**, 18849–18859.

[12] S. Yun, S. Hong, J. A. I. Acapulco, H. Y. Jang, S. Ham, K. Lee, Q4 S. K. Kim and S. Park, , 2015, **21**, 6165–6172.

[13] Z. Li, J. Nan, X. Zhang, S. Ye, H. Shen, S. Wang, L. Fang, P. Xue, J. Zhang and B. Yang, *J. Phys. Chem. C*, 2015, **119**, 11839–11845.

[14] W. Rechberger, A. Hohenau, A. Leitner, J. R. Krenn, B. Lamprecht and F. R. Aussenegg, *Opt. Commun*., 2003, **220**, 137–141.

[15] S.-Y. Ding, E.-M. You, Z.-Q. Tian and M. Moskovits, *Chem. Soc. Rev*., 2017, **46**, 4042–4076.

[16] K. Kneipp, H. Kneipp, V. Kartha, R. Manoharan, G. Deinum, I. Itzkan, R. Dasari and M. Feld, *Phys. Rev. E: Stat. Phys., Plasmas, Fluids, Relat. Interdiscip. Top*., 1998, **57**, 6281–6284.

[17] S. Shanmukh, L. Jones, J. Driskell, Y. P. Zhao, R. Dluhy and R. a. Tripp, *Nano Lett*., 2006, **6**, 2630–2636.

[18] R. A. Tripp, R. A. Dluhy and Y. Zhao, *Nano Today,* 2008, **3**, 31–37.

[19] M. Fleischmann, P. J. Hendra and A. J. McQuillan, *Chem. Phys. Lett.*, 1974, **26**, 163–166.

[20] D. L. Jeanmaire and R. P. Van Duyne, *J. Electroanal. Chem*., 1977, **84**, 1–20.

[21] J. P. Camden, J. A. Dieringer, J. Zhao and R. P. Van Duyne, *Acc. Chem. Res*., 2008, **41**, 1653–1661.

[22] M. Yang, R. Alvarez-Puebla, H. S. Kim, P. Aldeanueva-Potel, L. M. Liz-Marza´n and N. A. Kotov, *Nano Lett.*, 2010, **10**, 4013–4019.

[23] K. L. Wustholz, A. I. Henry, J. M. McMahon, R. G. Freeman, N. Valley, M. E. Piotti, M. J. Natan, G. C. Schatz and R. P. Van Duyne, , 2010, **132**, 10903–10910.

[24] J. Kumar, R. Thomas, R. S. Swathi and K. G. Thomas, *Nanoscale*, 2014, **6**, 10454–10459.

[25] H. Liu, Z. Yang, L. Meng, Y. Sun, J. Wang, L. Yang, J. Liu and Z. Tian, *J. Am. Chem. Soc*., 2014, **136**, 5332–5341.

[26] P. Taladriz-Blanco, N. J. Buurma, L. Rodriguez-Lorenzo, J. Perez-Juste, L. M. Liz-Marza´n and P. Herves, *J. Mater. Chem*., 2011, **21**, 16880–16887.

[27] Z. Qian and D. S. Ginger, *J. Am. Chem. Soc*., 2017, **139**, 5266–5276.

[28] P.-G. Yin, Y. Chen, L. Jiang, T.-T. You, X.-Y. Lu, L. Guo and S. Yang, *Macromol. Rapid Commun*., 2011, **32**, 1000–1006.
[29] L. Fillaud, M. M. Chehimi, J. Aubard, A. Hohenau and N. Felidj, *ACS Nano*, 2010, **4**, 6491–6500.
[30] L. Lin, X. Peng, M. Wang, L. Scarabelli, Z. Mao, L. M. Liz- Marza´n, M. F. Becker and Y. Zheng, *ACS Nano*, 2016, **10**, 9659–9668.
[31] X. Cheng, R. Sun, L. Yin, Z. Chai, H. Shi and M. Gao, *Adv. Mater.*, 2017, **29**, 1604894.
[32] Q.-H. Guo, C.-J. Zhang, C. Wei, M.-M. Xu, Y.-X. Yuan, R.- A. Gu and J.-L. Yao, *Spectrochim. Acta, Part A*, 2016, **152**, 336–342.
[33] F. Hu, H. Lin, Z. Zhang, F. Liao, M. Shao, Y. Lifshitz and S.- T. Lee, *Sci. Rep*., 2014, **4**, 7204.
[34] A. La Porta, A. Sa´nchez-Iglesias, T. Altantzis, S. Bals, M. Grzelczak and L. M. Liz-Marza´n, *Nanoscale*, 2015, **7**, 10377–10381.
[35] A. Okada, D. Nagao, H. Ishii and M. Konno, *Soft Matter*, 2012, **8**, 3442–3445.
[36] A. Okada, D. Nagao, T. Ueno, H. Ishii and M. Konno, *Langmuir*, 2013, **29**, 9004–9009.
[37] K. Watanabe, H. Ishii, M. Konno, A. Imhof, A. van Blaaderen and D. Nagao, *Langmuir*, 2016, **33**, 296–302.
[38] K. D. Hermanson, S. O. Lumsdon, J. P. Williams, E. W. Kaler and O. D. Velev, *Science*, 2001, **294**, 1082–1086.
[39] H. Ding, W. Liu, J. Shao, Y. Ding, L. Zhang and J. Niu, *Langmuir*, 2013, **29**, 12093–12103.
[40] B. C. Gierhart, D. G. Howitt, S. J. Chen, R. L. Smith and S. D. Collins, *Langmuir*, 2007, **23**, 12450–12456.
[41] N. G. Bastu´s, J. Comenge and V. Puntes, *Langmuir*, 2011, **27**, 11098–11105.
[42] B. Y. Enustun and J. Turkevich, *J. Am. Chem. Soc*., 1963, **85**, 3317–3328.
[43] Y. Q. He, S. P. Liu, L. Kong and Z. F. Liu, *Spectrochim. Acta, Part A*, 2005, **61**, 2861–2866.
[44] I. Blakey, Z. Merican and K. J. Thurecht, *Langmuir*, 2013, **29**, 8266–8274.
[45] T. Lou, Y. Wang, J. Li, H. Peng, H. Xiong and L. Chen, *Anal. Bioanal. Chem*., 2011, **401**, 333–338.
[46] A. Ramos, H. Morgan, N. G. Green and A. Castellanos, *J. Phys. D: Appl. Phys*., 1998, **31**, 2338–2353.
[47] A. Ramos, H. Morgan, N. G. Green and A. Casrellanos, *J. Colloid Interface Sci.*, 1999, **217**, 420–422.
[48] E. I. Izgorodina, M. Forsyth and D. R. MacFarlane, *Phys. Chem. Chem. Phys*., 2009, **11**, 2452–2458.
[49] M. Zahn, Y. Ohki, D. B. Fenneman, R. J. Gripshover and V. H. Gehman, *Proc. IEEE*, 1986, **74**, 1182–1221.
[50] A. von Hippel, *IEEE Trans. Electr. Insul.*, 1988, **23**, 801–816.
[51] A. Michota and J. Bukowska, *J. Raman Spectrosc*., 2003, **34**, 21–25.
[52] G. Lu, B. Shrestha and A. J. Haes, *J. Phys. Chem. C*, 2016, **120**, 20759–20767.
[53] L.-M. Chen and Y.-N. Liu, *ACS Appl. Mater. Interfaces*, 2011, **3**, 3091–3096.